北海道大学地球物理学研究報告
Geophysical Bulletin of Hokkaido University, Sapporo, Japan
No. 68, March 2005, pp. 11−29

Relationship between Micro-pressure Perturbation and Convective Activity Observed in the Orofure Mountain Range in Hokkaido, Japan

Koyuru IWANAMI
Advanced Technology Research Group, National Research Institute for Earth Science and Disaster Prevention, Tsukuba 305−0006, Japan
Katsuhiro KIKUCHI
Department of Biological Environment, Faculty of Bioresource Sciences, Akita Prefectural University, Akita 010−0195, Japan
Hiroshi UYEDA
Hydroshperic Atmospheric Research Center, Nagoya University, Nagoya 464−8601, Japan
and
Takashi TANIGUCHI
Hokkaido Head Office, Japan Weather Association, Sapporo 064−8555, Japan
(Received December 3, 2004)

Rainfall observations were carried out with a mobile weather radar, special mesoscale network of raingauges; wind vanes and anemometers; and microbarometers from late August to early September in 1985 and 1986 on the southeastern slope of the Orofure mountain range in the southwestern part of Hokkaido, Japan. The rainfalls on August 26 in 1985 were associated with a depression traveling eastward, and surface winds over the observation area were northerly. At that time the rainfall amount was distributed not only on the southeastern slope but over a wide area. The perturbation pressure with a period of about 3.6 hours and an amplitude of 0.2 to 0.4 hPa was derived from the application of spectral analysis and Chebyshev bandpass filter to microbarograph data. It was found that the derived perturbation pressure had characteristics of gravity waves by comparing it with surface rainfall, divergence and radar reflectivity. The observed gravity wave caused a convergence of (0.5 to 1.8) $\times 10^{-4}$ sec^{-1} which corresponded to the updrafts of 0.1 to 0.2 ms^{-1} in the lower layer. The phase velocity was estimated to be about 23 ms^{-1} toward south-southeast from observed data and it corresponded to the phase velocity of the gravity wave propagating on the 5.1 km stable layer which was estimated from a two-layer model. In this case, no effect of topography on the derived gravity waves and precipitation clouds was found, however, it was considered that the traveling of an internal gravity wave was one of the mechanisms which enhanced the rainfall amount.

I. Introduction

The orographic rainfall has been energetically studied to date, especially in the South Wales hills in the British Isles (Browning et al., 1975; Hill et al., 1981), in the Owase area in the Ki-i Peninsula (Takeda et al., 1976; Takeda and Takase, 1980), and in the Orofure mountain range in Hokkaido, Japan. It is generally accepted that the annual mean rainfall amount and the times of heavy rainfalls on Hokkaido Island are smaller than those in other districts in Japan. However, on the southeastern slope of the Orofure mountain range facing the Pacific Ocean in the southwestern part of Hokkaido, there is a relatively large annual mean rainfall and heavy rainfalls amount to more than 90 $mmday^{-1}$ occur three or four times per year (Takeda and Kikuchi, 1978). This area has been frequently subjected to floods and landslides arising from heavy rainfalls (Harimaya et al., 1981). If the mechanisms of heavy rainfalls are clarified, the flood and damage they result in could be reduced through adequate forecasts of rainfall.

Kikuchi and his group have studied the heavy rainfalls in this region since 1978. Konno and Kikuchi (1981) classified the horizontal distribution of rainfall amount into five types according to the locations where the maximum peak of rainfall amount was located based on the results of observations using their special mesoscale raingauge network. They clarified that the distribution patterns were mainly influenced by the wind direction in the lower layer. Konno et al. (1981) made the observations on the size distribution of raindrops at two observation sites simultaneously on the mountain range and on the seaside of the same area. The results of their observations suggested that the heavy orographic rainfalls in this range arose from a combination of the lower layer clouds caused by an uplifting of the warm and wet air from the Pacific Ocean on the southeastern slope of the range and the precipitation from the upper layer clouds of the synoptic scale disturbance moving from the southwest to the northeast over this region. The numerical experiments by Konno and Kikuchi (1981) and Kikuchi et al. (1988) supported this conclusion and Iwanami et al. (1988) clarified the enhancement of rainfall amount by the two-layer cloud structure model (Bergeron, 1965) through their radar observation.

Kikuchi et al. (1988) further pointed out the importance of the role of the horizontal convergence in the increase of rainfall amounts on the mountainous regions because the valley became narrower from the seaside to the mountain side. This was noted in the results of their observations and numerical experiments. Tobizuka and Harimaya (1989) made a case study of seaside rainfalls in which the maximum peak of rainfall amount was located in the seaside region. It was shown that seaside rainfall was formed through the process in

which echo cells developed rapidly on the southeastern slope after crossing over the ridge of the range by frictional convergence because of the discontinuity in the surface roughness. Iwanami et al. (1989) also reported seaside rainfall from the shallow convective precipitating clouds with echo tops lower than 3 km formed by a southeasterly flow of outbreak from the high pressure over the Okhotsk Sea. Iwanami et al. (1997) described the results of case studies of two heavy rainfall cases caused by the stratiform and convective precipitation clouds. Furthermore, the airflows in the precipitation clouds over the southeastern slope of the Orofure mountain range were estimated for the first time by the VVP method using Doppler velocity data gathered in the summer season in 1989 (Iwanami et al., 1998). It was demonstrated that effects of the topography were produced on the horizontal winds in the lower layer when the wind direction was east-southeast to south.

It is known that there are two kinds of phenomena treated as gravity waves. One has a period in the order of 10 minutes and the other several hours, but both their characteristic phase velocities exceed 50 $kmhr^{-1}$. It was suggested that the source mechanisms of gravity waves were severe thunderstorm activity, shear instability, large scale disturbances, etc. The short period pressure perturbations were studied by Curry and Murty (1974), Gedzelman and Rilling (1978), Bedard et al. (1986) and others. Gedzelman and Rilling (1978) showed that times of large-amplitude gravity waves frequently preceded the onset of cyclonic precipitation by some 12 to 24 hours while times of small-amplitude gravity waves usually indicated continuation of fair weather.

On the other hand, Eom (1975), Stobie et al. (1983) and Savage et al. (1988) studied the relationships between pressure perturbation with periods of 1 to 4 hours and convective activity. Matsumoto and Ninomiya (1965) derived mesoscale disturbance by using a pressure deviation from 2.5 hr running mean for the snowfalls in Hokuriku District in Japan. Uccellini (1975) analyzed gravity waves with about 3 hr period and 1 hPa amplitude, and pointed out that convective activity became strong after the passage of the wave trough. Koch and Golus (1988) dealt with the statistical determination of gravity wave characteristics through autospectral, perturbation map and cross spectral analyses. Further, internal gravity waves attracted attention as the formation mechanism of rainbands (Parsons and Hobbs, 1983). Koch et al. (1993) summarizes the results of detailed study from CCOPE of the vertical structure of mesoscale gravity waves that played a significant role in the generation of mesoscale convective convex.

In this paper, we describe the relationship between micro-pressure perturbation with a period of 3.6 hours and convective activity observed on August 26, 1985 in the Orofure mountain range in Hokkaido, Japan.

II. Observations

Our radar observations of rainfalls were carried out in the Orofure mountain range from late August to early September for about 3 weeks in 1985 and 1986, in combination with raingauges, wind vanes and anemometers, and microbarometers. Figure 1 shows the observation area and arrangement of instruments. The southeastern slope of the Orofure mountain range running nearly parallel to the coastline faces the Pacific Ocean from Tomakomai (Tentative site number of our observations: B-71) through Shiraoi (S-11), Noboribetsu (A-57) to Muroran (B-77), thus the orographic rainfalls caused by the orographic uplifting of the warm and wet southeasterly airflow from the Pacific Ocean occur frequently

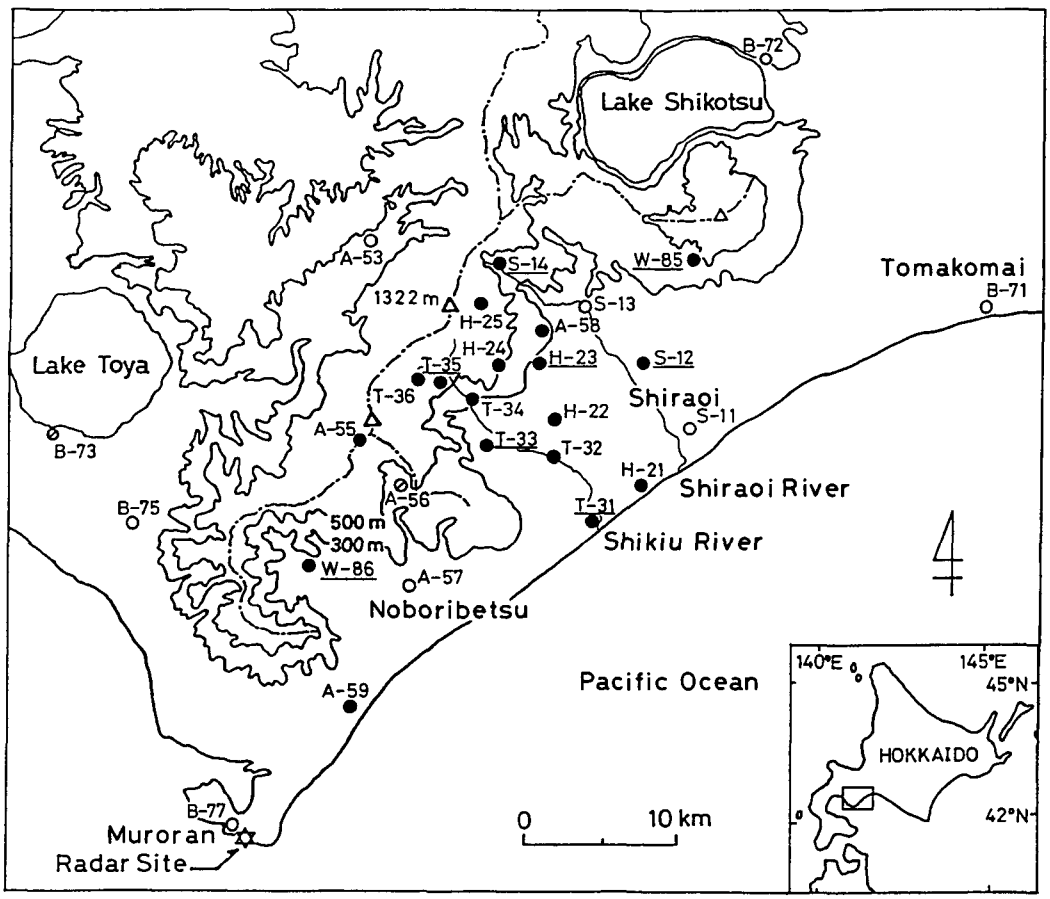

Fig. 1. Map of the observation area and arrangement of instruments. Contour curves have been drawn for 300 and 500 m a.s.l. The curving chained lines represent crestlines. Symbols of observation sites —○: meteorological observatory and AMeDAS supported by JMA, ∅: rainfall amount measuring robot supported by JMA, ●: raingauge supported by this work. Wind vanes and anemometers were set up at the sites underlined and microbarometers at S-11, S-13 and T-32.

in this area. In the figure, the locations of the meteorological observatories, AMeDAS and the rainfall amount measuring robots supported by the Japan Meteorological Agency (JMA), and of our 17 sites of raingauge of the tipping bucket long period automatic type (CMO-LRT 55) are represented by respective symbols. The locations of almost all raingauge sites were the same as that of the past observations (Konno and Kikuchi, 1981; Kikuchi et al, 1988). Further we set up 7 wind vanes and anemometers at the sites underlined to research airflow near the ground surface and 3 microbarometers (PD80HA, ST LAB., INC.) at S-11, S-13 and T-32 to investigate the relationship between convective activity and perturbation of surface air pressure for the first time in the observations in this area. A wind vane and anemometer at W-85 and a microbarometer at S-11 were set up only in 1985, and raingauges at A-59 and W-86 and wind vanes and anemometers at T-33 and W-86 only in 1986 to collect more data in the southwestern part of this area.

This observation network includes two valleys, that is, S-line along the Shiraoi River from Shiraoi (S-11) to the Shiraoi waterfall (S-14) and T-line along the Shikiu River from Takeura (T-31) to close to the watershed of Kushibetsu (T-36). The H-line from Hagino (H-21) to near Todomatsuzawa (H-25) was located on the ridge between the two lines described above. The A-53 site (Ohtaki-AMeDAS by JMA) is located on the northwestern slope of the Orofure mountain range.

The mobile weather radar of the Faculty of Science, Hokkaido University was set up on the cliff (118 m above the sea level) on the southeast side of Muroran City in order to watch the southeastern slope of the Orofure mountain range from that side in consideration of observation results in 1983 (Tobizuka and Harimaya, 1989). The radar had a 9,410 MHz frequency, 30 kW peak transmitting power and resolution of 250 m in radial and 1.0 degree in azimuthal direction, respectively. It was connected with the data processor and the three-dimensional digital data of precipitating clouds within 63.5 km range in radius could be obtained by volume scans consisting of several PPI (Plan Position Indicator) scans with elevation angle interval of 1.1 degree at every 10 minutes. The data were recorded on magnetic tapes after the elimination of the ground clutter by non-coherent MTI (Moving Target Indicator) method, the range correction and data averaging. Therefore, the distributions of the equivalent radar reflectivity factor could be displayed on PPI and CAPPI (Constant Altitude PPI) with 1 km×1 km grids and on the arbitrary vertical cross section with 1 km (horizontal)×0.5 km (vertical) grids in time of analyses.

III. Results

The surface weather charts at 09 and 21 JST on August 26 in 1985 are denoted in Fig. 2.

The depression with surface fronts over Primorskii at 09 JST moved east-southeastward and reached offshore Wakkanai at 21 JST on August 26. The rainfalls were associated with the low pressure system. According to the aerological data of Sapporo at 09 JST, convective unstable layer presented below 1.0 km a.s.l. and very humid atmosphere extended to 6.0 km. The surface wind direction at S-11 site was northwest to north-northwest and the effect of the topography on the precipitation clouds passing over the observation area was not recognized. The relationship between pressure perturbation and convective activity was found in this rainfall under such a situation.

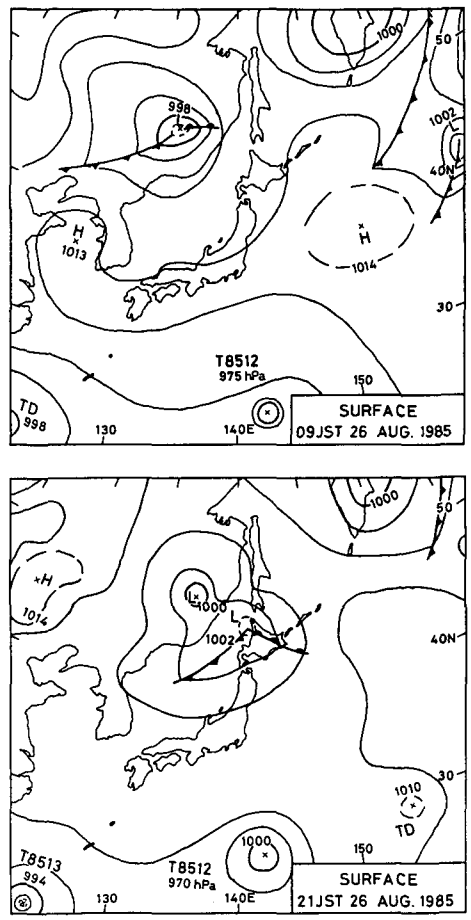

Fig. 2. Surface weather charts at 09 and 21 JST on August 26, 1985.

The horizontal distribution of the total rainfall amount for this case is shown in Fig. 3. The rainfall amount was distributed over a wide area including the northwest side of the Orofure mountain range and around the B-71 site but also over the southeastern slope of the mountain range. The maximum peak of rainfall amount extended laterally from T-36 to B- 71 site and it corresponded to the direction of the movement of the precipitation clouds. Although the southeasterly wind was remarkable at the B-71 site before 16 JST on August 26, the surface winds over the southeastern slope of the mountain range were calm or northerly.

Figure 4 shows the time series of the rainfall intensity for 20 minutes at four raingauge sites that recorded more than 70 mm for the day in the maximum peak area. These time series are arranged from west to east downward from the top of the figure. There were three rainfall periods, that is, 09−13 JST, 14−16 JST and 17−20 JST on August 26 recorded 2 to 4 mm per 20 minutes in intensity at each raingauge site, and the maximum intensity was 11 mm per 20 minutes at the S-12 site for 18:20−18:40 JST. These rainfalls were caused by the stratiform precipitation clouds. Figure 5 shows examples of the radar echoes passing over the observation area on the CAPPI pictures at 2.5 and 5.0 km a.s.l. calculated from the

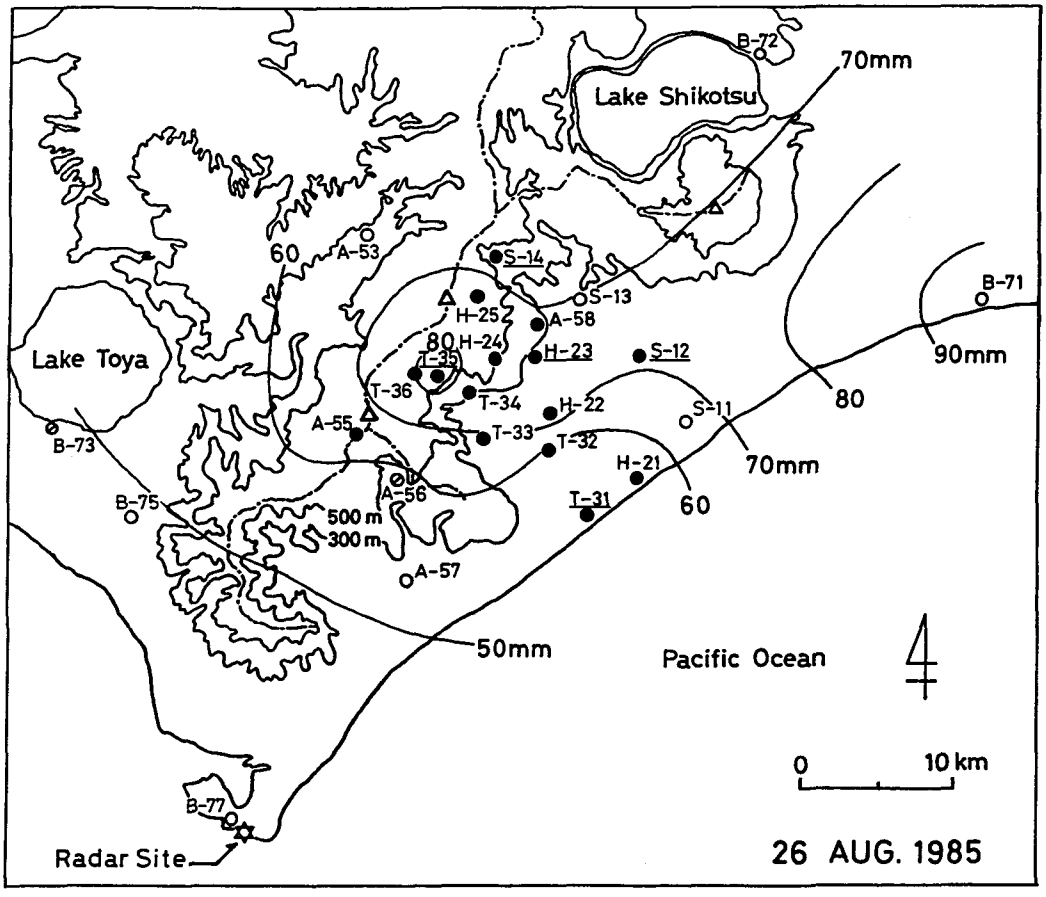

Fig. 3. Horizontal distribution of total rainfall amount on August 26, 1985. The contours of rainfall amount are drawn at 10 mm intervals from 50 mm.

PPI series recorded for 14:20−14:28 JST on August 26, 1985. It is found that these stratiform precipitation clouds had horizontal dimensions of more than 100 km and active echo areas stronger than 30 dBZ, and that they moved mostly eastward.

In order to derive the perturbation pressure from the microbarograph data, the following method was adopted. The sensibility of the microbarometer used is 0.1 hPa, and data sampling interval was selected as 5 minutes because the perturbation period of interest was at minimum longer than 30 minutes. The top panel of Fig. 6 shows the time evolution of surface pressure at the S-11 and T-32 sites. Unfortunately, the pressure data could not be recorded at the S-13 site on the day due to difficulties. These time series contain synoptic-scale trends, diurnal and semidiurnal tides and higher-frequency oscillations, and they must be removed in order to extract the perturbation pressure of interest. The frequency range from 0.2 to 1.2 cycles per hour (denoted by cph, hereafter), that is, a period range from 50 minutes to 5 hours, was selected as the object of analysis taking into consideration the time

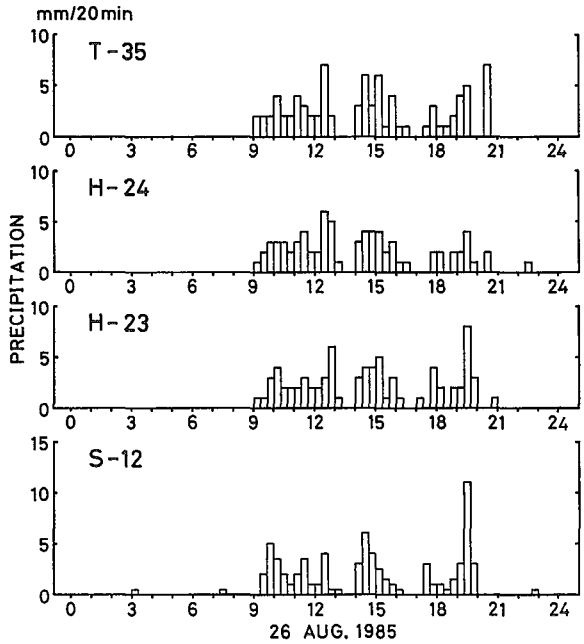

Fig. 4. Time series of rainfall intensity per 20 min at the sites of T-35, H-24, H-23 and S-12.

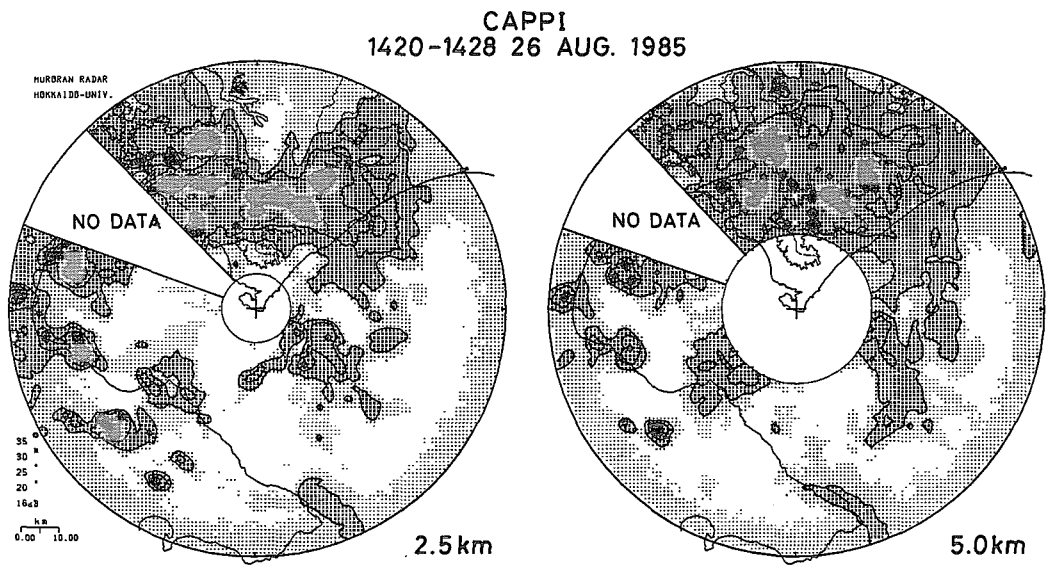

Fig. 5. CAPPI pictures at 2.5 km (left) and 5.0 km (right) a.s.l. for 14:20−14:28 JST on August 26, 1985. The echo intensities are indicated by both contours at 5 dBZ intervals from 20 dBZ and symbols shown on the lower left of the figure. The outer and inner circles of each panel show maximum range of 63.5 km and no data areas. The coastline, crestline and contours of 300 m a.s.l. are drawn by slightly thick solid, thin dashed and thin solid lines, respectively.

evolutions of rainfall intensity as shown in Fig. 4 and making reference to the past studies of the relation of gravity waves with convection. For the purpose of extracting this range of perturbation, the Chebyshev bandpass filter whose cut-off periods were 45 minutes and 6 hours was applied to the pressure deviation from time average value of sampled data. The response curve of the filter is represented in the bottom panel of Fig. 6. The Chebyshev bandpass filter is a kind of recursive digital filter (Saito, 1978).

The top panel in Fig. 7 shows the time series of perturbation pressure derived from the application of the bandpass filter whose response was shown in Fig. 6. The peak-to-peak amplitudes of the perturbations were counted as 0.4 to 1.0 hPa and several kinds of oscillations are found in those time series. The power spectra of the perturbation pressures were calculated and shown in the bottom panel of Fig. 7. The abscissa and ordinate represent frequency in units of cph and power spectrum, and the bandwidth of Parzen's spectral window used here for smoothing and 95 % confidence interval are indicated by the horizontal and perpendicular bars on the upper right of panel. Accounting for the bandwidth and confidence interval, the spectral peak was considered significant only when it was common

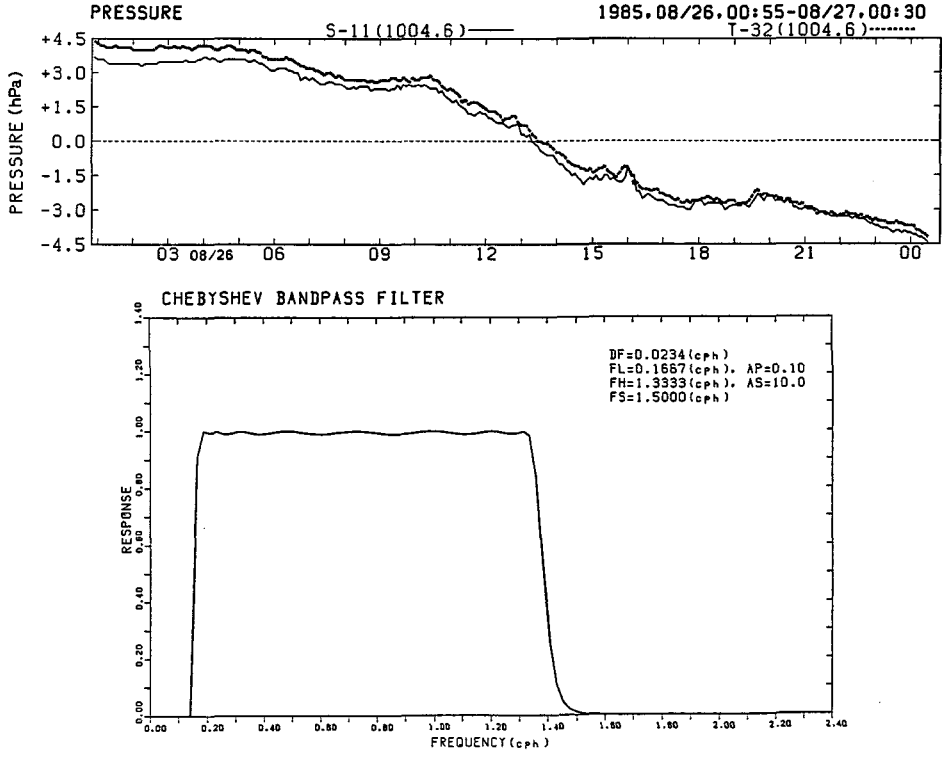

Fig. 6. Time series of pressure at S-11 and T-32 sites indicated by solid and thick dashed lines (top), and the response curve of the used Chebyshev bandpass filter (bottom). The center of the pressure axis denotes 1004.6 hPa in the top panel, and the abscissa of the bottom panel represents the frequency in units of cycles per hour (cph).

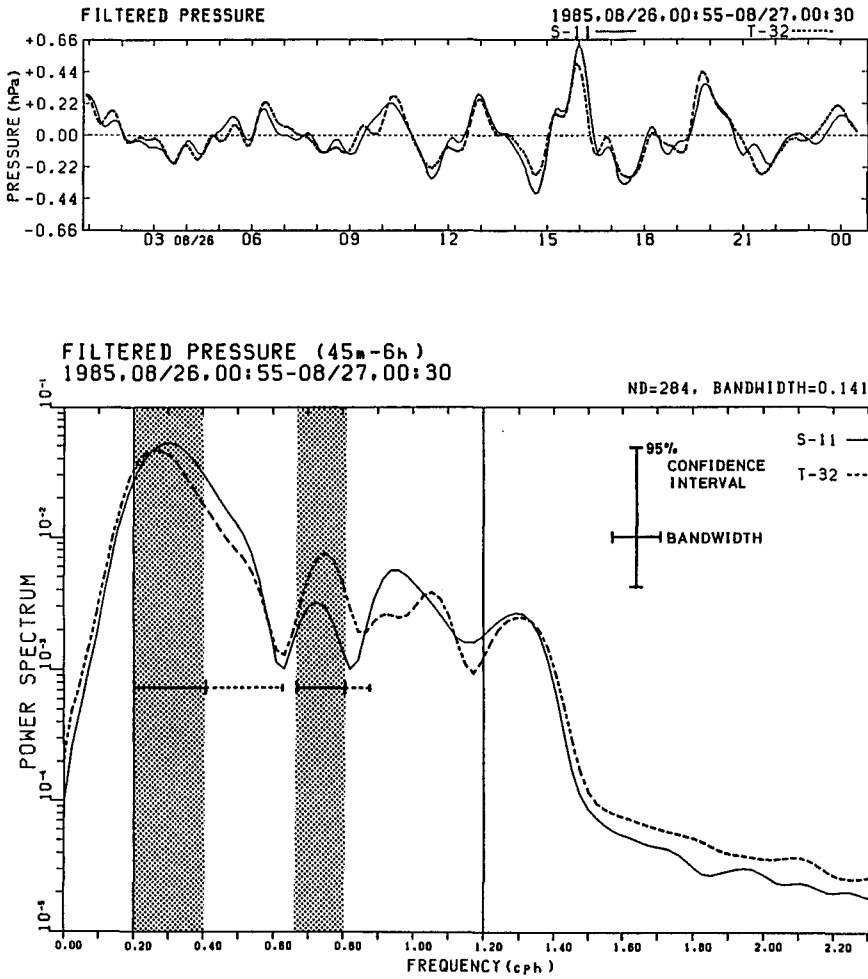

Fig. 7. Time series of perturbation pressure derived from the application of the first-step bandpass filter shown in Fig. 6 to pressure at the S-11 and T-32 sites (top) and the power spectra of the perturbation pressure shown in top panel (bottom). The solid and thick dashed lines correspond to the S-11 and T-32 data in both panels. See text.

to both S-11 and T-32 sites, and the frequency of the peak was included in the range from 0.2 to 1.2 cph (period from 50 minutes to 5 hours) drawn by long vertical lines in the panel. In this case, two spectral peaks with frequency (period) centered on about 0.28 cph (3.6 hours) and 0.74 cph (1.4 hours) were selected, and the similar Chebyshev bandpass filters with the passband indicated by the horizontal bars and stippled areas were applied to the original surface pressure data.

Figure 8 shows the perturbation pressure derived from application of the second-step bandpass filters, whose respective passbands ranged from 0.2 to 0.41 cph and from 0.67 to 0.81cph, to the original pressure data. Time series in the top and bottom panels represent

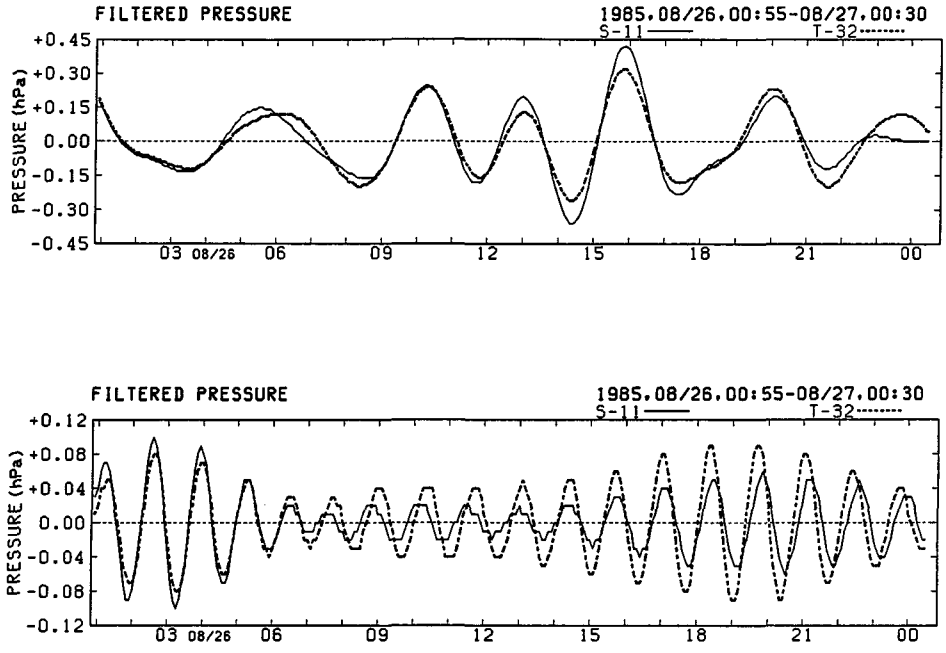

Fig. 8. Time series of perturbation pressure derived from application of two kinds of second-step bandpass filters to the S-11 (solid lines) and T-32 data (thick dashed lines).

the perturbation pressures with the period around 3.6 and 1.4 hours, respectively. The peak-to-peak amplitudes of these were found to be 0.3 to 0.8 hPa and 0.1 to 0.2 hPa. Attention to the pressure perturbation of an approximately 3.6 hr period is given hereafter because a relationship was recognized between the pressure perturbation and the time series of rainfall intensity.

Figure 9 represents a schematic vertical cross section of the pressure and wind speed associated with propagating gravity waves with no basic current (Eom, 1975; Bosart and Sanders, 1986). When a linear plane gravity wave propagates toward right with phase speed C on a boundary such as a temperature inversion or an isentropic surface at the altitude of H, the distributions for the surface pressure crest (HIGH) and trough (LOW) and wind velocities (arrows) are expected as in the figure. Further, it is expected that divergence (DIV) and convergence (CON) areas are formed behind the surface pressure crest and trough, respectively, and that updrafts are produced and convective activity (clouds illustrated schematically) is enhanced in the convergence area. These expectations for the phase relations between gravity waves and divergence and convective activity are compared with the observation results.

The perturbation pressure (solid line in the middle panel) at the S-11 site is compared with the time series of radar reflectivity (top panel), filtered divergence (dotted line in the

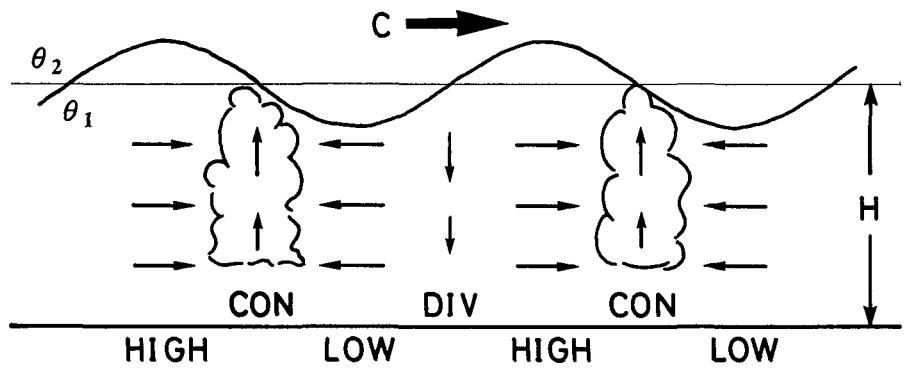

Fig. 9. Idealized vertical cross section of a linear plane gravity wave propagating toward the right with phase speed, C on the boundary at height of H. Distributions for the surface pressure crest and trough, and air flows are indicated by HIGH and LOW, and arrows. DIV and CON show the expected divergence and convergence areas and regions of convective activity are schematically illustrated by clouds.

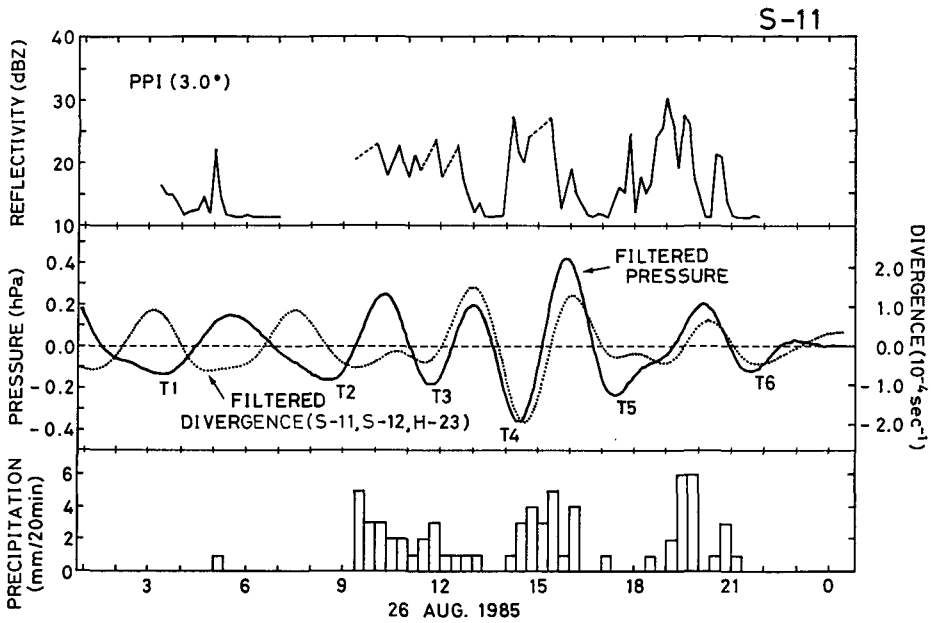

Fig. 10. Time series of reflectivity above S-11 on 3.0 degree PPI (top), perturbation pressure and surface divergence derived from the application of the second-step bandpass filter (middle), and rainfall intensity per 20 min (bottom) at S-11 site. Time series of the perturbation pressure and perturbation divergence are drawn by the solid and dotted line, respectively.

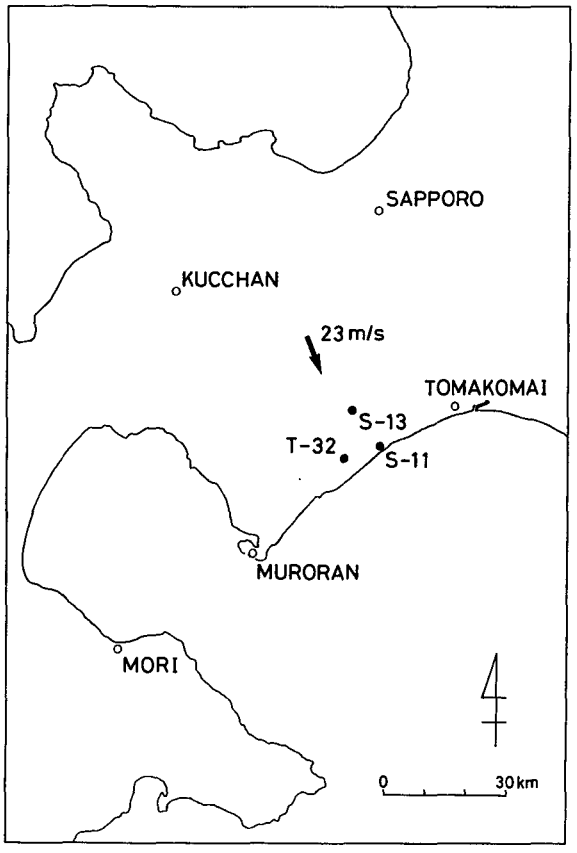

Fig. 11. Map of the surrounding barometer sites used for the phase velocity calculations. The solid and open circles indicate the locations of our microbarometer sites and meteorological observatories supported by JMA, respectively. The arrow shows the derived phase velocity of the observed gravity wave.

middle panel) and 20 min rainfall intensity (bottom panel) in Fig. 10. The radar reflectivity values were selected on a 1 km×1 km mesh of PPI image at the elevation angle of 3.0 degree, with altitude corresponded to 2.2 km a.s.l. at S-11 site. The filtered pressure (left ordinate) has been already shown in the top panel of Fig. 8 and filtered divergence (right ordinate) was derived from the application of the same bandpass filter with pressure to the divergence values in the triangle area enclosed by S-11, S-12 and H-23 sites calculated from 10 min mean winds. This was examined to determine whether the expected relationship from the model of gravity waves could be satisfied. It was found that six perturbation pressure troughs (T1 to T6) passed over the site. It was also found that the convergence values reached extremes, reflectivity became stronger, and surface rainfall began to be recorded after the troughs T1, T2 and T5 passed. The intensification of radar echo and rainfall followed at the trough T4, although divergence changed similarly with pressure. It is assumed that the trough T3 did not satisfy the expected relationship, since rainfall continued before the trough T3 passed and downdrafts associated with rainfall influenced the surface pressure and divergence. From the examination, the expected relationship from a two-layer model of gravity waves was

satisfied at the S-11 site where convergence and convective activity became stronger and rainfall was observed after the passing of a perturbation pressure trough. Further a similar relation was recognized at the T-32 site. It is therefore considered that the perturbation pressure with a period of about 3.6 hours and an amplitude of 0.2 to 0.4 hPa derived from the application of a bandpass filter had characteristics of internal gravity waves, and that the gravity waves became one of the mechanisms for rainfall enhancement in the observation area under some weather situations. Although similar analyses were applied for six other rainfall cases during the observation period in 1985 and 1986, remarkable spectral peaks did not appear on the power spectra or it was shown that perturbation pressure did not have such a relationship with time series of rainfall intensity.

IV. Discussion

The phase velocity of the observed gravity waves could not be estimated by using microbarograph data alone because of the trouble with the microbarometer at S-13 and the small arrangement range of our microbarometers. Thus, the estimation was carried out

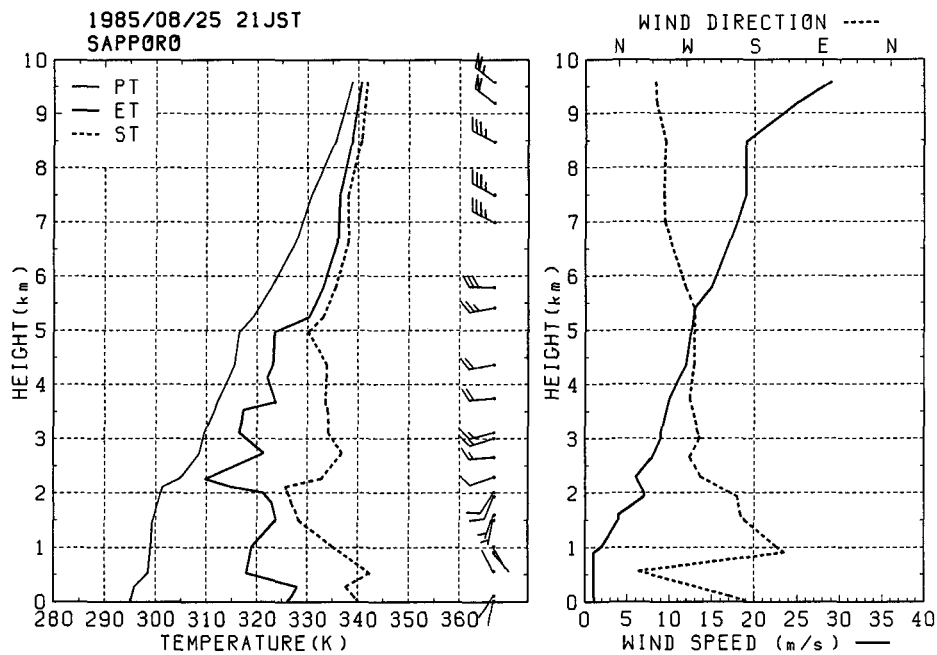

Fig. 12. Left panel: Vertical profiles of potential temperature (thin solid line), equivalent potential temperature (thick solid line) and saturated equivalent potential temperature (dashed line) at Sapporo. Wind velocities are also indicated by flag (20 ms^{-1}), full barb (5 ms^{-1}) and half barb (2.5 ms^{-1}). Right panel: Vertical profiles of wind direction (dashed line) and speed (solid line) above Sapporo at 21 JST on August 25, 1985.

using data of two microbarographs and 1 day period automatic aneroid barometers at the meteorological observatories of JMA shown in Fig. 11. At that time the phase velocity was estimated to be about 23 ms^{-1} (that is, about 83 kmh^{-1}) toward south-southeast as indicated by an arrow in the figure by means of calculations of the time lag (Gedzelman and Rilling, 1978) and the phase of cross spectra (Koch and Golus, 1988) from surface observations. This value of phase speed is larger than 50 kmh^{-1} in common with results reported by many investigators.

The sounding results are shown in Fig. 12 in Sapporo at 21 JST on August 25. The stable layers existed at 0.4, 2.2 and 5.1 km a.s.l. and they were candidates of the boundary in Fig. 9. The expected phase speeds through the air of gravity waves from the two-layer model as shown in Fig. 9 were calculated by

$$C=[(\theta_2-\theta_1)gH/\theta_2]^{1/2}, \tag{1}$$

where θ represents potential temperature and subscripts 1 and 2 indicate the values of a lower and upper layer of boundary (Bosart and Sanders, 1986). The calculated values were 6, 15 and 21 ms^{-1} and wind components toward south-southeast were 1, -1 and 3 ms^{-1} at respective stable layer at 0.4, 2.2 and 5.1 km a.s.l. The phase speeds over the ground estimated from eq. (1) and corrected for advection by the horizontal wind resolved along the observed direction of the height of the stable layer were 7, 14, and 24 ms^{-1} at respective candidate. It was inferred that the observed wave was the gravity waves propagating toward south-southeast on a stable layer at 5.1 km a.s.l.

The updrafts, to begin with, should exist for the beginning of convective activity, condensation of water vapor, formation and growth of precipitation particles and occurrence of heavy rainfalls. The passing of a gravity wave also causes an upward motion in the atmosphere. The convergence values which resulted from the gravity wave with a period of 3.6 hours as indicated in Fig. 10 were $(0.5 \text{ to } 1.8)\times10^{-4}$ sec^{-1} and they corresponded to the updrafts of 0.1 to 0.2 ms^{-1}, for example, at the height of 1.0 km. The updraft values caused by the passing of the observed gravity wave were smaller than those produced by forced uplifting, estimated as the potential flow for the observation area by the method of Nakatsugawa et al. (1990). But these updraft values were larger than the updraft accompanied by synoptic scale disturbances (Matsumoto, 1974) and comparable to or slightly smaller than those resulting from horizontal convergence mainly caused by orographic features such as valleys (Iwanami et al., 1989).

V. Conclusions

Rainfall observations were carried out with a mobile weather radar and special meso-scale network of raingauges; wind vanes and anemometers; and microbarometers from late August to early September in 1985 and 1986 on the southeastern slope of the Orofure mountain range in the southwestern part of Hokkaido, Japan. The rainfalls on August 26 in 1985 were associated with a depression traveling eastward and surface winds over the observation area were northerly. At that time the rainfall amount was distributed over a wide area. The perturbation pressure with a period of about 3.6 hours and amplitude of 0.2 to 0.4 hPa was derived from the application of spectral analysis and Chebyshev bandpass filter to microbarograph data. It was found that the derived perturbation pressure had characteristics of gravity waves by comparing the perturbation pressure with surface rainfall, divergence and radar reflectivity. That is to say, the surface convergence became large, and the reflectivity above became strong and rainfall was observed at the ground after the passage of perturbation pressure trough. The observed gravity wave caused a convergence of $(0.5 \text{ to } 1.8)\times10^{-4}$ sec^{-1} and it corresponded to the updrafts of 0.1 to 0.2 ms^{-1} in the lower layer. The phase velocity was estimated to be about 23 ms^{-1} toward south-southeast from data of our microbarographs and aneroid barometers at the surrounding meteorological observatories after JMA. This corresponded to the expected phase velocity of the gravity wave propagating on the 5.1 km stable layer estimated from a two-layer model. Although similar analyses were applied for six other rainfall cases in 1985 and 1986, remarkable spectral peaks did not appear on the power spectra or it was shown that perturbation pressure did not have such a relationship with time series of rainfall intensity. In this case, no effect of topography on the derived gravity waves and precipitation clouds was found, however, it was considered that the traveling of an internal gravity wave was one of the mechanisms which enhanced the rainfall amount. And it is speculated that under suitable conditions the effects of topography might be produced in precipitation clouds. Such a relationship between perturbation pressure and convective activity was however not clear.

Acknowledgments The authors would like to express their sincere thanks Prof. T. Harimaya and Dr. Y. Asuma, Meteorological Laboratory, Department of Geophysics, Faculty of Science, Hokkaido University, for their valuable discussion/advice and students in the laboratory for their support in this field work. And thanks are also due to Sapporo District Meteorological Observatory, Muroran Local Meteorological Observatory and Tomakomai Weather Station by JMA for their generous offering of useful data. This study

was carried out as a link in the chain of the program of the JSPS Fellowships for Japanese Junior Scientists (K.I.). A part of the expense for this research was supported by a Grant-in-Aid for Research in Natural Disasters "Studies on the Generation Mechanisms of Local Heavy Rainfalls on the Southeastern Slope of Orofure Mountain Range in Hokkaido Island, Japan" (Project No. 61025001) and for the encouragement of Young Scientists (K.I.) (No. 02952103) of the Ministry of Education, Science and Culture of Japan.

References

Bedard, Jr., A. J., F. Canavero and F. Einaudi, 1986. Atmospheric gravity waves and aircraft turbulence encounters, *J. Atmos. Sci.*, **43**, 2838−2844.

Bergeron, T., 1965. On the low-level redistribution of atmospheric water caused by orography, *Suppl. Proc. Int. Conf. Cloud Phys.*, Tokyo, May 1965, 96−100.

Bosart, L. F. and F. Sanders, 1986. Mesoscale structure in the megalopolitan snowstorm of 11−12 February 1983. Part III: A large-amplitude gravity wave, *J. Atmos. Sci.*, **43**, 924−939.

Browning, K. A., C. W. Pardoe and F. F. Hill, 1975. The nature of orographic rain at wintertime cold fronts, *Quart. J. R. Met. Soc.*, **101**, 333−352.

Curry, M. J. and R. C. Murty, 1974. Thunderstorm-generated gravity waves, *J. Atmos. Sci.*, **31**, 1402−1408.

Eom, J. K., 1975. Analysis of the internal gravity wave occurrence of 19 April 1970 in the Midwest, *Mon. Wea. Rev.*, **103**, 217−226.

Gedzelman, S. D. and R. A. Rilling, 1978. Short-period atmospheric gravity waves: A study of their dynamic and synoptic features, *Mon. Wea. Rev.*, **106**, 196−210.

Harimaya, T., K. Kikuchi, T. Endoh and N. Horie, 1981. Damage caused by the heavy rainfall in the southwestern part of Hokkaido Island on August 1980, *Geophys. Bull. Hokkaido Univ.*, **40**, 113−126 (in Japanese with English abstract).

Hill, F. F., K. A. Browning and M. J. Bader, 1981. Radar and raingauge observations of orographic rain over South Wales, *Quart. J. R. Met. Soc.*, **107**, 643−670.

Iwanami, K., K. Kikuchi and T. Taniguchi, 1988. A possible rainfall mechanism in the Orofure mountain range Hokkaido, Japan −The rainfall enhancement by a two-layer cloud structure−, *J. Meteor. Soc. Japan*, **66**, 497−504.

Iwanami, K., K. Kikuchi and T. Taniguchi, 1989. A case study of heavy rainfalls from the shallow orographic precipitating clouds in the Orofure mountain range, Hokkaido, Japan, *J. Fac. Sci., Hokkaido Univ., Ser. VII (Geophysics)*, **8**, 281−299.

Iwanami, K., K. Kikuchi, H. Uyeda and T. Taniguchi, 1997. Two case studies of heavy rainfalls from the stratiform and convective precipitation clouds in the Orofure mountain range, Hokkaido, Japan, *J. Fac. Sci., Hokkaido Univ., Ser. VII (Geophysics)*, **10**, 239−268.

Iwanami, K., K. Kikuchi, H. Uyeda and T. Taniguchi, 1998. Airflow circulation in the precipitation clouds over the southeastern slope of the Orofure mountain range, Hokkaido, Japan, *J. Fac. Sci., Hokkaido Univ., Ser. VII (Geophysics)*, **11**, 185−205.

Kikuchi, K., N. Horie, T. Harimaya and T. Konno, 1988. Orographic rainfall events in the Orofure mountain range in Hokkaido, Japan, *J. Meteor. Soc. Japan*, **66**, 125−139.

Koch, S. E. and R. E. Golus, 1988. A mesoscale gravity wave event observed during CCOPE. Part I: Multiscale statistical analysis of wave characteristics, *Mon. Wea. Rev.*, **116**, 2527−2544.

Koch, S. E., F. Einaudi, P. B. Dorian, S. Lang and G. M. Heymsfield, 1993. A mesoscale gravity wave event

observed during CCOPE. Part IV: Stability analysis and Doppler-derived wave vertical structure, *Mon. Wea. Rev.*, **121**, 2483−2510.

Konno, T. and K. Kikuchi, 1981. Properties of local heavy rainfall on the southeast slope of Orofure mountain range in the Iburi District, Hokkaido, Japan, (I) −Distribution patterns of rainfall amount−, *Geophys. Bull. Hokkaido Univ.*, **39**, 1−18 (in Japanese with English abstract).

Konno, T., K. Kikuchi, K. Wakahara and K. Suzuki, 1981. Properties of local heavy rainfall on the southeast slope of Orofure mountain range in the Iburi District, Hokkaido, Japan, (II) −Simultaneous observations of the size distribution of rain drops at two raingauge stations−, *Geophys. Bull. Hokkaido Univ.*, **39**, 19−35 (in Japanese with English abstract).

Matsumoto, S., 1974. Dynamics and structure of the mesoscale disturbances, *Technical Report of JMA*, **86**, 136−149 (in Japanese).

Matsumoto, S. and K. Ninomiya, 1965. Meso-scale disturbance observed in the vicinity of a cold vortex center −With special regards to gravity waves−, *Pap. Met. Geophys.*, **XVI**, 9−22.

Nakatsugawa, M., M. Takemoto and T. Yamada, 1990. Rainfall characteristics in catchment area (3) − Simulation of wind and rainfall in mountainous area−, *Mon. Rep. Civil Engineering Res. Inst.*, **447**, 20−35 (in Japanese with English abstract).

Parsons, D. B. and P. V. Hobbs, 1983. The mesoscale and microscale structure and organization of clouds and precipitation in midlatitude cyclones. XI: Comparisons between observational and theoretical aspects of rainbands, *J. Atmos. Sci.*, **40**, 2377−2397.

Saito, M., 1978. An automatic design algorithm for band selective recursive digital filters, *Geophysical Exploration*, **31**, 240−263 (in Japanese with English abstract).

Savage, M. L., G. A. Weidner and C. R. Stearns, 1988. A diagnostic study of the influence of a gravity wave upon regional weather, *Mon. Wea. Rev.*, **116**, 347−357.

Stobie, J. G., F. Einaudi and L. W. Uccellini, 1983. A case study of gravity waves −convective storms interaction: 9 May 1979, *J. Atmos. Sci.*, **40**, 2804−2830.

Takeda, E. and K. Kikuchi, 1978. Local heavy rainfalls in Hokkaido Island, Japan (I) −On the contribution of heavy rainfalls to the annual amount of rainfalls−, *Geophys. Bull. Hokkaido Univ.*, **37**, 19−29 (in Japanese with English abstract).

Takeda, T., N. Moriyama and Y. Iwasaka, 1976. A case study of heavy rain in Owase area, *J. Meteor. Soc. Japan*, **54**, 32−41.

Takeda, T. and K. Takase, 1980. Radar observation of rainfall system modified by orographic effects, *J. Meteor. Soc. Japan*, **58**, 500−516.

Tobizuka, K. and T. Harimaya, 1989. A case study of seaside rainfall in the Iburi District, Hokkaido, *Geophys. Bull. Hokkaido Univ.*, **52**, 77−88 (in Japanese with English abstract).

Uccellini, L. W., 1975. A case study of apparent gravity wave initiation of severe convective storms, *Mon. Wea. Rev.*, **103**, 497−513.

北海道オロフレ山系で観測された微気圧変動と対流活動の関係

岩波　越

防災科学技術研究所防災基盤科学技術研究部門

菊地　勝弘

秋田県立大学生物資源科学部生物環境学科

上田　博

名古屋大学地球水循環研究センター

谷口　恭

(財)日本気象協会北海道支社

(2004年12月3日受理)

1985年と1986年の8月下旬から9月上旬にかけて，北海道南西部のオロフレ山系南東斜面で，可搬型気象レーダーと独自の雨量計，風向風速計，微気圧計ネットワークを用いて降雨観測を行った．1985年8月26日の降雨は東に移動する低気圧に伴うものであったが，観測域の地上風は北寄りで，南東斜面だけでなく広範囲に降雨が分布した．

微気圧計データにスペクトル解析及びChebyshevのバンドパス・フィルターを適用し，周期が約3.6時間，振幅が0.2～0.4 hPaの微気圧変動を抽出した．地上の降雨量，発散量やレーダー反射強度と比較したところ，この微気圧変動は重力波の特徴を持っていた．すなわち，微気圧変動の谷の通過後に，地上付近の収束量が大きくなり，上空のレーダー反射強度が強まって，地上で降雨が観測された．この重力波による収束量は$(0.5\sim1.8)\times10^{-4}\mathrm{sec}^{-1}$，下層の上昇流は0.1～0.2 ms^{-1}であった．独自の微気圧計及び周囲の気象官署の気圧計の観測データから，位相速度は南南東に約23 ms^{-1}と見積もられた．この値は二層モデルから推定される高さ5.1 km付近に存在した安定層を伝搬する重力波の位相速度に対応していた．

観測期間中の他の6つの降雨事例についても同様の解析を行ったところ，微気圧計データのスペクトルに顕著なピークが現れないか，ピークは存在しても微気圧変動と地上の降雨量や発散量の時間変化との間に重力波と推測される関係は認められなかった．

1985年8月26日の事例では重力波や降水雲への地形の影響は認められなかったが，内部重力波の通過が降雨量増幅の一つの機構として働いていたと考えられる．